Q. J. R. Meteorol. Soc. (2004), **1**, pp. 1–40 doi: 10.1256/qj.yy.n

Identifiability of climatological air-sea fluxes by 4D-Var assimilation of seasonal hydrographic data

By C. Deltel[1*], H. Mercier[2], A. T. Weaver[3] and P. Delecluse[4]
[1]*LODYC, Paris, France*
[2]*LPO, Brest, France*
[3]*CERFACS, Toulouse, France*
[4]*LSCE/CEA, Gif-sur-Yvette, France*

SUMMARY

Inaccurate air-sea fluxes are a major source of error in numerical ocean model simulations. The ocean is a key actor in the climate system, and any estimation procedure leading to improved geophysical forcing fields is thus of potential benefit. Variational estimation methods can yield theoretically optimal corrections to any model parameters, given appropriate observations of the ocean state. We have investigated the optimization of air-sea forcing fields using a 4D-Var method applied to a South Atlantic configuration of the OPA ocean general model. The ability of this assimilation system to improve climatological air-sea fluxes is examined in the idealised context of identical twin data experiments. In particular, we define the notion of parameter identifiability and try to establish the identifiability of surface fluxes during the austral summer. We first show that seasonal hydrographic data can be used to identify the seasonal mean heat and freshwater fluxes, separately or jointly, whereas they are less effective at reconstructing intraseasonal variability. Retrieving the wind stress from hydrographic data is a much more difficult task. Seasonal mean zonal stress can be properly recovered in the subtropical gyre and in coastal upwelling areas, but the westerly winds are erroneously reconstructed. Furthermore, meridional stress cannot be recovered, even partially. These results suggest that seasonal mean hydrological data are not effective in constraining the seasonal mean wind stress field. This inverse estimation problem is ill-posed in the proposed setting. A stronger result is that a perfectly known wind stress field can be remarkably degraded to balance a heat flux estimation error. Limitations related to the present configuration are discussed, as well as extensions of our conclusions to real data experiments.

KEYWORDS: Air-sea fluxes Estimation Variational assimilation

1. INTRODUCTION

The advent of satellites and worldwide *in situ* observation programs such as the World Ocean Circulation Experiment (WOCE) has resulted in a large amount of data over the last decade, which show that state-of-the-art numerical models often fail to represent accurately reality. This is not acceptable to understand the past ocean circulation, and possibly to predict some components of its evolution, especially with a view to climate monitoring.

The quality of a simulated ocean trajectory mainly depends on the model physics, particularly its parametrisations of unresolved physical processes, and on the accuracy of both initial conditions and geophysical surface forcing fields. Assimilation methods have been developed which can take into account available datasets to improve model trajectories. For example, four-dimensional variational assimilation (4D-Var) has been used for many years in meteorology and oceanography to optimize model initial conditions to give an improved fit to observations.

By contrast, air-sea surface flux optimisation remains much less explored, especially in idealised contexts which allow us to clarify the method's strengths and limitations in a perfectly known framework. The heat flux inverse problem is the best documented. Gaspar *et al.* (1990) estimated the turbulent heat fluxes using the evolution of the thermal content of a one-dimensional (1D) oceanic mixed layer model, as observed with sea surface temperature (SST) data. The same 1D model was used by Roquet *et al.* (1993) who implemented a 4D-Var scheme to estimate heat flux from temperature

* Corresponding author: Laboratoire d'Océanographie Dynamique et de Climatologie (LODYC), University Pierre et Marie Curie, Paris, France.

profile data. Yuan and Hsueh (1998) and Yuan and Rienecker (2003) also estimated heat flux by assimilating SST data, with a 4D-Var algorithm applied to a linear thermodynamical submodel. Zhu *et al.* (2002) explored the ill-posed nature of this problem by assimilating high frequency upper ocean temperature data in a different 1D model to estimate heat forcing at various temporal resolutions. Concerning the wind stress estimation problem, Bonekamp *et al.* (2001) showed that tropical wind stress could be improved over a two month assimilation window by assimilating a dense temperature dataset (Tropical Ocean-Atmosphere) using 4D-Var. They attributed this result to the fast equatorial dynamics. Recently, Stammer *et al.* (2002) estimated all air-sea fluxes as well as initial conditions of temperature and salinity using the 1992-1997 assimilation window, by 4D-Var assimilation of Levitus monthly mean hydrography, Reynolds monthly SST, and sea level anomaly maps in a global ocean general circulation model (OGCM).

However, systematic twin data experiments have never been performed to assess how well air-sea fluxes may be recovered, either separately or jointly, *via* a 4D-Var method applied to an OGCM. To explore this problem, we have developed an ocean 4D-Var system aimed at improving air-sea fluxes by means of a regional model-data synthesis. In this paper, we explore the optimal results that can be obtained from a 4D-Var estimation of air-sea fluxes, given no *a priori* knowledge of the sought after fields, and by assimilation of simulated seasonal mean hydrographic data. Following Navon (1997), any of the fluxes is said to be identifiable (or not) by the data if it can be properly reconstructed. We begin to investigate identifiability by exploring the sensitivity of model counterparts of the observations to surface fluxes. The stronger this sensitivity, the better their identifiability by the data. Moreover, these experiments provide insight into underlying physical processes by which the assimilation method corrects air-sea fluxes to reduce model-data discrepancies.

This paper is organized as follows. In section 2, we describe the South Atlantic model configuration implemented for this study. The estimation problem and the assimilation system are also described. A spin-up integration of the model provides synthetic (twin) data for the assimilation experiments. The twin data are defined as a seasonal mean of simulated model hydrology in order to mimic the information content in available climatologies such as Reynaud *et al.* (1998).

In sections 3 and 4, we explore the extent to which forcing information can be extracted from the data. Section 3 is devoted to the determination of thermohaline fluxes. In section 4, wind stress is added to the control variable. A summary and conclusions are given in section 5.

2. METHOD AND MODEL

(*a*) *Model configuration and spin-up.*

Due to the high computational burden associated with 4D-Var, we chose to concentrate on the South Atlantic basin. In the framework of the CLIPPER modeling project, a French contribution to WOCE, model configurations with different spatial resolutions have been implemented in the whole Atlantic domain from Antarctica to 70°N. The OGCM OPA 8.1 was used Madec *et al.* (1998). Details about the Atlantic configurations can be found in CLIPPER (2001). In the present study, our limited area model is essentially a subdomain of the CLIPPER low resolution configuration. The horizontal grid is a Mercator isotropic grid with resolution 1° at the equator. The meridional extent of the domain ranges from 16°S, inspired from the MOCA model (Barnier *et al.* 1998), to 71°S, to avoid problems in the assimilation algorithm associated with ice. The zonal

extent ranges from 72°W to 31°E. The vertical grid has 43 geopotential levels with a tight spacing (less than 15m) for 8 levels near the surface.

A horizontal Laplacian operator is used for lateral mixing of tracers and momentum (K_h =2000 m^2/s). The vertical mixing of momentum and tracers is calculated using a 1.5 turbulent closure model based on a prognostic equation for turbulent kinetic energy (TKE) and a closure assumption for the turbulent length scales (Blanke and Delecluse (1993), Madec *et al.* 1998). A no-slip boundary condition is applied along the coastlines, and non-linear friction is applied at the bottom.

Open boundaries are defined at Drake Passage and at 30°E between Africa and Antarctica. Because of the Antarctic Circumpolar Current (ACC), with a transport of the order of 140 Sverdrup (1 Sverdrup $= 10^6\, m^3/s$), the choice of these boundaries is extremely important for the circulation of the South Atlantic (Treguier *et al.* 2001)). We preferred implementing a fixed open boundary condition (OBC) rather than a radiative boundary condition to avoid differentiating a threshold process in constructing the adjoint model. In contrast, the boundary at 16°S is modelled as a coastline surrounded by a thick buffer zone (6 grid points, with relaxation times ranging from 3 days to 100 days) where water masses can be recycled. This choice is compatible with the net northward transport across the Atlantic, which is close to zero. A similar southern boundary was chosen at 71°S for the same reason.

The surface forcing fields are derived from the European Centre for Medium-Range Weather Forecasts (ECMWF) reanalysis ERA-15 (Gibson *et al.* 1997, Garnier *et al.* 2000). To reduce the dimensionality of the flux estimation problem, we define the forcing fields by linear interpolation between monthly mean fields from an ERA-15 climatological year (*i.e.* 15 year mean).

The hydrological seasonal climatology of Reynaud *et al.* (1998) is used to initialize the model, and as relaxation fields in the buffer zones by linear interpolation to the model time. The Southern Hemisphere summer data serve as initial conditions, because other seasons are worse sampled. This configuration has been integrated for 9 years starting from rest. During this spin-up, surface temperatures and salinities are relaxed toward Reynaud *et al.* (1998) climatology to prevent surface fields from drifting too much from observed values. Figure 1 shows the resulting mean stream function, which is quite similar to that obtained by Treguier *et al.* (2001) for a higher resolution configuration of the global Atlantic basin. In particuliar this shows that our choice of a closed boundary at 16°S is reasonable to the modeled basin.

(*b*) *The 4D-Var assimilation system.*

Following standard notations (Ide *et al.* 1997), we denote $\mathbf{x}$ the vector of model initial conditions, $\mathbf{x}^b$ the corresponding background state, and $\mathbf{y}^\circ$ the vector of space and time distributed observations. 4D-Var aims at optimizing model input parameters such as initial conditions $\mathbf{x}$ to fit simultaneously $\mathbf{x}^b$ and $\mathbf{y}^\circ$ in a statistically weighted least squares sense. This is achieved by minimizing a cost function, which takes the form:

$$\mathcal{J}(\mathbf{x}) = \underbrace{\frac{1}{2}(\mathbf{x}-\mathbf{x}^b)^\top \mathbf{B}_{(\mathbf{x})}^{-1}(\mathbf{x}-\mathbf{x}^b)}_{\mathcal{J}_b} + \sum_{i=0}^{n} \underbrace{\frac{1}{2}(\mathcal{H}(\mathbf{x}(t_i))-\mathbf{y}_i^\circ)^\top \mathbf{R}_i^{-1}(\mathcal{H}(\mathbf{x}(t_i))-\mathbf{y}_i^\circ)}_{\mathcal{J}_{o,i}} \quad (1)$$

where n is the number of time steps within the assimilation window, $\mathbf{x}(t_i) = \mathcal{M}(t_i, 0)(\mathbf{x})$ is the model state vector at time t_i, obtained by integration of the direct model $\mathcal{M}$ (described above) from initial state $\mathbf{x} = \mathbf{x}(0)$ up to time t_i. $\mathbf{B}_{(\mathbf{x})}$ is the background error covariance matrix, and $\mathbf{R}$ denotes the observation error covariance matrix, including the

contribution from representativeness error (Lorenc 1986). $\mathcal{H}$ is the observation operator, mapping the state vector space into observation space. The gradient of the observational cost function, needed to iteratively bring to zero the cost function's gradient $\nabla\mathcal{J}(\mathbf{x})$, makes use of the adjoint model $\mathbf{M}^\top$, where $\mathbf{M} \cong (\partial\mathcal{M}/\partial\mathbf{x})|_{\mathbf{x}=\mathbf{x}^b}$ is the tangent linear (TL) model. The specific approach chosen in the OPA-VAR assimilation system is of incremental type (Courtier *et al.* 1994, Courtier 1997). It is fully described in Weaver *et al.* (2003) (WVA hereafter), and we recall briefly it main characteristics.

Assuming the required correction is small enough, one can integrate the increment *via* the TL model instead of integrating the updated control vector by help of the full non-linear model $\mathcal{M}$. The underlying assumption is known as the TL hypothesis. The cost function is then approximate but quadratic, which ensures the existence and uniqueness of a minimum, and ensures numerical efficiency of the iterative minimization algorithm.

The main drawback of this formulation is that model-data misfits are linearly approximated about the same background state. Courtier *et al.* (1994) suggested a pragmatic approach for accounting for weak nonlinearities by occasionnaly updating the reference trajectory during the minimization process. The operators **M** and **H** (TL of $\mathcal{H}$) are then linearized about this new reference trajectory. The update of the trajectory and the computation of the innovation vector are performed on the outer loops, using increments calculated within inner minimization loops.

In practice, the vertical physics in the direct model is simplified before linearization, because the TKE algorithm is highly nonlinear and discontinuous. The vertical diffusivities are held constant during the inner iterations, and are taken from the reference trajectories. A similar approximation was made by Yuan and Rienecker (2003). Zhu *et al.* (2002) discuss higher order variants of this approximation and show that such modified TL models allow us to improve predictability by help of linearized dynamics and thus to enlarge the assimilation window. They indeed show that the linearized physical processes may fail to represent major feedback loops – and associated saturation with time – between the nonlinear processes, thus leading to exponential growth of initial perturbations.

(*c*) *South Atlantic configuration of the assimilation system.*

(i) *Climatological observation operator.*

This investigation uses idealized observations. However, the dataset we would ultimately like to assimilate consists of the Reynaud *et al.* (1998) Atlantic seasonal climatological atlas of temperature and salinity, which is representative of a mean historical seasonal cycle of the basin. If N denotes the number of time steps over one season, and if we assume to simplify notations that all state variables are observed, the seasonal atlas incremental cost function takes the form:

$$\mathcal{J}_o^{inc}(\delta\mathbf{x}) = \frac{1}{2}\left\{\left(\frac{1}{N+1}\sum_{i=0}^{N}\mathbf{M}(t_i,0)\,\delta\mathbf{x}\right)-\mathbf{d}\right\}^\top \mathbf{R}^{-1}\{...\} \tag{2a}$$

$$\text{whose gradient reads:}\quad \nabla\mathcal{J}_o^{inc}(\delta\mathbf{x}) = \sum_{i=0}^{N}\mathbf{M}(t_i,0)^\top\left(\frac{\mathbf{R}^{-1}\mathbf{d}}{N+1}\right). \tag{2b}$$

The latter expression shows that the adjoint forcing associated with the climatological innovation $\mathbf{d} = \mathbf{y}^\circ - \frac{1}{N+1}\sum_{i=0}^{N}\mathbf{x}^b(t_i)$ is a constant fraction of the weighted innovation. Note that the observational constraint requires the TL approximation to be valid over

an assimilation window as large as three months, the validity of which will be justified later.

(ii) *Optimization of air-sea fluxes.*

So as to estimate the climatological seasonal air-sea net heat flux Q, the freshwater flux $E-P$, and the wind stress $\boldsymbol{\tau}=(\boldsymbol{\tau}_x,\boldsymbol{\tau}_y)$, we added them to the control variables. For the heat flux estimation problem, one may wish to distinguish solar and nonsolar components in the estimation procedure. However, the evolution of the mixed layer thermal content is driven by the net heat flux, so that inverting both components from mixed layer data would lead to an ill-posed problem Roquet *et al.* (1993).

A three-month assimilation window, as discussed above, requires four monthly forcing fields for linear interpolation. We therefore define an extended control vector:

$$\delta\mathbf{z}=(\delta\mathbf{x}^\top,\delta\mathbf{q}^\top)^\top \tag{3a}$$

$$\text{with:}\quad \delta\mathbf{q}=(\delta\mathbf{q}_1^\top,\delta\mathbf{q}_2^\top,\delta\mathbf{q}_3^\top,\delta\mathbf{q}_4^\top)^\top \tag{3b}$$

$$\text{and:}\quad \delta\mathbf{q}_k=({\delta Q_k}^\top,{\delta(E-P)_k}^\top,{\delta\boldsymbol{\tau}_k^x}^\top,{\delta\boldsymbol{\tau}_k^y}^\top)^\top,\qquad k=1,...,4 \tag{3c}$$

The new incremental cost function reads:

$$\mathcal{J}^{inc}(\delta\mathbf{z})=\frac{1}{2}\,\delta\mathbf{z}^\top\mathbf{B}_{(\mathbf{z})}^{-1}\delta\mathbf{z}\;+\;\mathcal{J}_o^{inc}(\delta\mathbf{z}) \tag{4}$$

where $\mathcal{J}_o^{inc}(\delta\mathbf{z})$ has the same expression as before with an additional dependance on $\delta\mathbf{q}$. Its gradient makes use of the adjoint fields of the input forcings. The extended background error covariance matrix $\mathbf{B}_{(\mathbf{z})}$ is taken to be block diagonal, and its forcing part $\mathbf{B}_{(\mathbf{q})}$ is purely diagonal in the current implementation. Note however that the linear interpolation formulation may be interpreted as a time correlation constraint for the heat flux.

(*d*) *Formulation of the estimation problem.*

An estimation problem is well-posed if (i) it possesses a solution, (ii) this solution is unique, (iii) this solution is stable, *i.e.* depends continuously on the observations. The concept of parameter identifiability refers to points (i) and (ii), and can be formulated as the one-to-one property of mapping from observation space to parameter space (Kitamura and Nakarigi 1977, Goodson and Polis 1979, Chavent 1979; see Navon 1997 for a review). In our situation, the relationship between parameters to estimate and observations is defined by a combination of the ocean model and the seasonal-mean observation operator. If we denote by $\mathcal{G}$ the generalized observation operator (parameter-to-observations mapping), the problem is actually to invert the equation $\mathcal{G}(\mathbf{q})=\mathbf{y}^\circ$, where $\mathbf{q}$ are the required unknown parameters. As our focus will be on air-sea fluxes, $\mathbf{q}$ will denote in turn heat flux, freshwater flux, windstress, and combinations of them. However, as $\mathcal{G}$ includes an OGCM integration, it cannot be inverted analytically, and we have to design a numerical strategy to try to obtain some insight into the question of identifiability.

From now on, the control vector is taken to be only $\delta\mathbf{q}$, *i.e.* we ignore errors in the initial conditions, $\delta\mathbf{x}=0$. The assimilation problem then has O(10^5) forcing degrees of freedom to be estimated from p =O(5.10^5) hydrological observations. Denoting by $\mathbf{G}$ the TL of $\mathcal{G}$ about the background $\mathbf{q}^b$, the problem reads $\mathbf{G}\;\delta\mathbf{q}=\mathbf{d}$ within the first outer loop, where $\mathbf{d}=\mathbf{y}^\circ-\mathcal{G}(\mathbf{q}^b)$ is the innovation vector. The incremental 4D-Var cost function takes the form:

$$\mathcal{J}^{inc}(\delta\mathbf{q})=\frac{1}{2}\;\delta\mathbf{q}^\top\;\mathbf{B}_{(\mathbf{q})}^{-1}\;\delta\mathbf{q}+\frac{1}{2}\;(\mathbf{G}\;\delta\mathbf{q}-\mathbf{d})^\top\mathbf{R}^{-1}\;(\mathbf{G}\;\delta\mathbf{q}-\mathbf{d}). \tag{5}$$

The minimizing solution $\mathbf{q}^a$ exists and is uniquely defined because of $\mathcal{J}_b$, even if $\mathbf{q}$ is not identifiable by the data, *i.e.* whenever $\mathbf{G}$ is not invertible. On the contrary, were identifiability ensured, both the true physical solution $\mathbf{q}^t$ and the 4D-Var analysis $\mathbf{q}^a$ would coincide within observational error.

A straightforward way to investigate sensitivity and thus identifiability is to explore the way the model equivalent to the observations is modified in response to a change in parameter space. In this paper, we will qualitatively explore this sensitivity with the assumption that no *a priori* information about the fluxes is available. To introduce this inside the assimilation system, we set minimisation starting points and background values to zero. The background uncertainties will be chosen large enough so as to downplay the role of the background term ($\mathbf{B}^{-1}$ is close to zero in some sense). If the fluxes are indeed identifiable by the data, this choice should not be critical to the solution. The sensitivity study to any given flux then consists of assessing the latter's impact on the ocean trajectory by turning if off in a "free" simulation (forced and free simulations are hereafter denoted by $(+)$ and $(-)$, respectively).

3. IDENTIFIABILITY OF THERMOHALINE FLUXES BY HYDROLOGICAL DATA

(*a*) *Experimental strategy.*

The austral summer season of the ninth year of the spin-up is considered as the *true* ocean state. No noise is added to the observations, since we are interested in determining the information contained in the data in the most favorable situation. No relaxation to observed SST and sea surface salinity (SSS) is used in the assimilation system. Were they activated, model-data misfits due to flux misspecification would be substantially reduced without the need to improve input fluxes. In this section, we shall investigate the separate and then the joint identifiability of heat and freshwater fluxes.

Let us describe in detail the heat flux experiment $\mathbf{q} \equiv Q$ (analogous for the freshwater experiment). The background heat flux is set to zero $Q^b \equiv 0$, which physically means that air and sea do not exchange any heat in the background integration. The associated background error covariance matrix $\mathbf{B}_{(Q)}$ is diagonal with constant variance σ_Q^2. In order to be large enough, σ_Q is arbitrarily defined as four times the standard deviation of the true flux $\sigma_Q = 4 \times 80 = 320\text{W/m}^2$. Strictly speaking, such a situation is beyond the validity of estimation theory Lorenc (1986) because the true summer flux has a nonzero mean $\overline{Q^t} = 50\text{W/m}^2$, while no bias is theoretically allowed. The observational error covariance matrix $\mathbf{R}$ is defined to be 1/10-th of a realistic mean vertical T ans S error profile deduced from Reyanud *et al.* (1998). This corresponds to an observational uncertainty of about 0.03°C (resp. 5.10^{-3} p.s.u.) in the upper 100m ocean depth, decreasing down to 0.02°C (resp. 2.10^{-3} p.s.u.) at 500m depth, and then to 5.10^{-3} °C (resp. 10^{-3} p.s.u.) below 1000m.

(*b*) *Model sensitivity to heat flux.*

The surface boundary condition for potential temperature θ leads to a heating rate given by $\partial\theta/\partial t = Q/(\rho\, C_p \Delta z)$ for a water column of height Δz, where ρ and C_p are the density and specific heat of seawater. Over the summer, the ocean mainly gains heat from the atmosphere. A constant 50W/m^2 flux over Δz =50 meters increases sea temperature by 2°C in three months. The $\overline{\theta^+} - \overline{\theta^-}$ surface temperature map (Fig. 2a) shows indeed variations ranging on the order of 2°C mainly confined to 50m depth (not shown). Note that this behaviour cannot be representative of winter convection, which makes the impact of strongly negative heat flux patterns penetrate much deeper into the

ocean. In contrast, surface salinity and mean horizontal velocity are much less sensitive to heating, with variations of the order of 10^{-2} p.s.u. and 5 mm/s respectively.

The temperature sensitivity map shows qualitative agreement with the corresponding heat forcing field (Fig. 2a,b). To first order, this may indicate that the heat flux acts upon the ocean surface in a local linear way by modifying its thermal content, other physical processes like horizontal advection or diffusion being negligible. However, there are noticeable sensitivity patterns that seem to contradict this suggestion. One striking feature is that the sensitivity clearly vanishes along the austral open boundaries. Close to the Drake Passage, the incoming ACC advects prescribed water masses, and thus diminishes any physical sensitivity to surface exchanges with the atmosphere. Moreover, neither the Brazil/Falklands Confluence region (55°W,45°S) nor the Benguela upwelling (12°E,25°S) area seem to agree with this local heating interpretation. These surface considerations thus suggest that ocean dynamics may play an important role in those regions. This can be further assessed by means of the local one-dimensional evolution equation for the water column thermal content, which makes it possible to calculate an equivalent seasonal mean heat flux $\overline{Q_{EQ}}$. Denoting by h the water depth impacted by the heating, this instantaneous equivalent flux can be expressed as the difference of thermal content between $(+)$ and $(-)$; it takes the form $Q_{EQ}(t) = \rho\, C_p\, \frac{\partial}{\partial t} \int_{-h}^{0} [\theta^+ - \theta^-]\, dz$. Assuming $Q_{EQ}(t)$ to be linear in time over the season, it can be conveniently written $Q_{EQ}(t) = \overline{Q_{EQ}} + \frac{\Delta Q}{T_a}(t - \frac{T_a}{2})$, where $\Delta Q = Q4 - Q1$ is the heat flux variation over the seasonal assimilation window T_a. Integrating from time 0 to t and taking the seasonal average yields the desired mean equivalent flux:

$$\overline{Q_{EQ}} = \frac{2\,\rho\, C_p}{T_a} \int_{-h}^{0} (\overline{\theta^+} - \overline{\theta^-})\, dz + \frac{\Delta Q}{6} \quad . \tag{6}$$

In the above expression $\Delta Q/6$ is O(-30W/m^2), so that $Q_{EQ}(t)$ could not have been taken constant in time. Note that h should best correspond to the oceanic mixed layer depth to retrieve heat fluxes by thermal content estimation Gaspar *et al.* (1990). Our resulting flux (Fig. 2c) with constant h is however well correlated with truth, with a maximum correlation of 0.82 being reached for $h =$ 42m (4-th model level). Still, local discrepancies over strong dynamical regions are similar to the sensitivity patterns discussed in the sensitivity map (Fig. 2a). This supports the previous suggestion that nonlinear dynamics can play a significant role in the way the heat flux impacts the water column.

An additional advantage of this simple $\overline{Q_{EQ}}$ computation is that it shows in a very simple, yet physical, way that the mean heat flux is actually identifiable by our mean hydrological data, since (6) is a linear inverse of the **G** operator. Furthermore, a small ocean depth and no salinity data were used to achieve this result. However, an important limitation of the conclusions in this section is that they are configuration dependent, and may not be entirely approporiate in more nonlinear models. Keeping this in mind however, one can now be optimistic about the variational heat flux retrieval discussed in the next section.

(*c*) *Seasonal heat flux identifiability.*

(i) *Convergence of the minimization.*

The normalized cost function $\frac{2}{p}\mathcal{J}^{inc}$ reaches a minimum value of 0.75 (Fig. 3a), which is less than its statistical expectation of 1 (Bryson and Ho 1975). This corresponds

to a reduction by 171 of the background cost value, after 18 iterations. However, the minimal state seems to be reached within a few inner iterations since the first outer update (iteration 6) yields a cost already close to the minimum value. When estimating heat flux from SST data, Yuan and Rienecker (2003) also report that most of their optimization takes place in the first 5 iterations, after which further decrease is difficult to obtain. The efficiency of this convergence is closely related to the existence of a direct linear relationship between the observed thermal content evolution and the surface heating expressed in (6). The surface temperature residuals have a slightly negative mean value -0.03°C, with a standard deviation 0.07°C almost twice as large as the prescribed observational error 0.04°C. This is probably due to the strong biases in our background setting Talagrand (1998), but the residuals match fairly well the assumed Gaussian error distribution (Fig. 3b).

(ii) *The optimal mean heat flux.*

The mean of the heat flux analysis increment δQ^a is shown in Fig. 2d. Its correlation with the true forcing fields reaches 0.92. Compared to the thermal content method (Eq. 6), the estimated fluxes are enhanced in the strongly dynamical regions, and now look similar to truth. This demonstrates the superiority of the 4D-Var method, which takes dynamics into account in reconstructing the heat flux.

This good agreement is modulated by a relatively large r.m.s. error of 17W/m^2. As suggested by residual satistics, the latter may be due to the strong bias imposed in the background state. Using a 4D-Var method in identical twin data experiments, Zhu *et al.* (2002) tried to recover the nonsolar heat flux over a few days from a background obtained by shifting the truth with a bias of 90W/m^2. They assimilated simulated temperature observations every 30min at high vertical resolution. Their r.m.s. estimation error is as large as ours, which they attribute to the ill-posed nature of the inverse heat flux problem.

Some noise also occurs in the dynamically sensitive regions discussed above, with geographical scales close to the model resolution. This may be due to the effects of nonlinearities, which may violate the TL approximation over the three month integration window used here, and lead to isolated poor values of the incremental gradient. This may also indicate a stability issue, a common feature associated with ill-posed inverse problems (Tichonov 1963, Navon 1997, Zhu *et al.* 2002). In other terms, large analysis error can be attributed to locally noisy estimates of the unknown fields. However, this problem does not appear critical in our situation, and could be efficiently solved by smoothing the increment by introducing non diagonal terms (correlations) in $\mathbf{B}_{(\mathbf{q})}$. If not fundamental in the current study, the introduction of correlations within the flux background error specification would be needed for more realistic studies, as is typically done when controlling initial conditions (see *e.g.* WVA and Weaver and Courtier (2001).

We conclude that the seasonal mean heat flux is identifiable by seasonal mean hydrological data. Even if this conclusion may be conditioned by the above limitations, there is no doubt that such data contain pieces of information appropriate to constrain the mean air-sea heat flux within the inverse system.

(*d*) *Intraseasonal heat flux retrieval.*

No subseasonal information is contained in our twin data. However, fluxes are controlled monthly, and one could thus hope to retrieve intraseasonal variability features by combining constraints from data and model dynamics. Some features of this reconstructed history are indeed encouraging. The monthly increments are reasonably well correlated with truth (0.69, 0.93, and 0.65), as illustrated in their zonal means

(Fig. 4). Amplitudes are poorly retrieved mainly since they are biased, and this may be related to the poor background state in our experiment. We can therefore conclude that some part of the intraseasonal variability has been retrieved. This result is necessarily achieved using the model dynamical constraints, which highlights a strength of the 4D-Var framework.

A noticeable feature is that the fourth field hardly deviates from its background value. This can be explained by its short impact on the ocean trajectory (one month), while memory from previous heat flux fields are kept at least two months by the system. As a consequence, the last field's contribution must be redistributed over the previous ones, which can not be expected to be highly reliable.

(*e*) *Freshwater flux and joint thermohaline fluxes identifiability.*

In our rigid lid model, the freshwater flux is introduced as a virtual salt flux $SSS \times (E - P)$ which immediately impacts the ocean surface salinity in a linear local way similar to the influence of heat flux on temperature discussed in section *(b)*. Therefore, the freshwater flux is expected to have a weak impact on temperature, which indeed is the case (not shown). The identifiability of seasonal and intraseasonal freshwater fluxes (Fig. 5) turns out to be similar to thoses obtained for the heat flux in the previous sections.

Moreover, joint estimation of heat and freshwater fluxes leads to increments that are similar to those obtained when the fluxes were estimated separately (not shown). We conclude that mean thermohaline fluxes are jointly identifiable by our data. The explanation for this result is given by the absence of cross sensitivity of both controls upon observed quantities in the present situation; *i.e.*, to first order, the heat flux only influences temperature, and the freshwater flux only influences salinity. The assimilation system thus does not have any other choice to fit the observations than to adjust the fluxes as it did in the separate estimation experiments. This means that the heat flux is only constrained by temperature observations and that the freshwater flux is only constrained by salinity observations in our configuration. Although temperature and salinity data were both assimilated, only the temperature information was actually used to optimize the heat flux, and only the salinity information was used to optimize the freshwater flux. This was further confirmed by the failure of an additional experiment (not shown) where we tried to estimate heat flux retaining salinity data only.

(*f*) *Discussion.*

We could probably have obtained the same results with less data. It is likely that mixed layer temperature observations or maybe even only SST data would be sufficient to properly constrain the heat flux, as suggested by our thermal content computation or by mixed layer models Zhu *et al.* (2002). Our results suggest that upper ocean salinity data probably constrain the freshwater flux in a similar way. Furthermore, it is presumably not necessary to estimate these fluxes with high horizontal resolution for climate studies since relevant patterns have large horizontal scales. Therefore horizontal data density could be relaxed, even if dynamically sensitive areas still probably need to remain better sampled. Yet the observing network structure would then be reflected on the resulting increments, unless the $\mathbf{B}_{(\mathbf{q})}$ matrix is improved by introducing autocorrelations in both the background heat and freshwater errors.

In contrast, recovering intraseasonal history obviously requires better observational time sampling than provided by a seasonal climatological dataset. SST data and ARGO profiles sample the water column thermal content and its variability at high frequency,

and look therefore to be a most promising dataset to estimate heat flux. Freshwater flux estimation would also benefit from the use of future global SSS data; *e.g.* from the satellite SMOS mission (Font *et al.* 2000). However, the choice of zero background fluxes is probably critical to our results, and it is likely that a reduced background bias would improve the estimations. Note that in real data experiments, background heat fluxes are better known, and only corrections to them are sought. This may reduce the problem of estimating the fluxes in the last month of the assimilation window.

However, the results obtained in this section demonstrate that our data can effectively constrain the thermohaline fluxes, and that it is worth moving to real data applications (see Deltel (2002)).

4. CAN HYDROLOGICAL DATA LEAD TO WIND IDENTIFIABILITY?

(*a*) *Wind stress identifiability.*

In our assimilation system, to estimate the wind stress $(\boldsymbol{\tau}_x, \boldsymbol{\tau}_y)$ is *a priori* a more difficult problem than to estimate heat and freshwater fluxes. While the number of data remains unchanged, there are twice as many unknowns as when each of the thermohaline fluxes was estimated. Moreover, wind stress acts upon ocean currents through a boundary condition so that their effects upon hydrological fields results from nonlinear heat and freshwater advection by Ekman transport or pumping. It is thus not obvious that indirect data of this kind can allow for wind stress identifiability, a question we now investigate.

As before, we begin by exploring ocean sensitivity to wind stress fields. Comparison of $(+)$ and $(-)$ trajectories shows that the wind stress generates currents over the uppermost three grid levels (figure not shown), indicating a model Ekman layer depth of about $\delta_{Ek} = 35$m. As expected, the associated transport perturbation $\Delta\mathbf{M} = \int_{-\delta_{Ek}}^{0} (\overline{\mathbf{u}^+} - \overline{\mathbf{u}^-})\, dz$ is oriented to the left of, and nearly perpendicular to the wind direction (Fig. 6a). In addition, the zonal integral $\int_{west}^{east} \Delta\mathbf{M}(x,y)\, dx$ correlates with the theoretical transport $\int_{west}^{east} \frac{-\boldsymbol{\tau}_x(x,y)}{\rho_0 f(y)}\, dx$ given by Ekman theory by more than 0.99 (Fig. 6c). The numerical ocean response to wind stress forcing is thus fully explained by Ekman theory, which in turn suggests how assimilation will be able to work to bring the model nearer to observations.

South of $40°$S, heat advection is principally due to horizontal Ekman transport. Westerly winds give rise to strong northward Ekman transport, cooling down the Ekman layer δ_{Ek} up to 3°C (Fig. 6b). This cooling is in agreement with the northward SST gradient in $(-)$ and an advective $3°$ latitude meridional scale, roughly computed from maximal Ekman velocities (4cm/s at $50°$S). Moreover, upward Ekman pumping $w_{Ek} = \mathrm{curl}_z\, \frac{\boldsymbol{\tau}}{\rho_0 f}$ = O(10^{-6}m/s) over one season gives an estimated 10m advective vertical scale (close to one model level), which explains the cooling observed beneath the surface cold tongue anomaly (green in Fig. 6b). Finally, noticeable water downwelling occurs (Fig. 6a,b) along the south-eastern coast of the basin, caused by local easterly wind patterns.

The ACC barotropic flow is prescribed by the OBC algorithm and is thus independant of the wind stress. This is not realistic however, since the ACC properties are substantially determined by the wind forcing. Note that the Sverdrup balance is unlikely to be valid in the Southern Ocean: the ACC characteristics are set by a complex interplay between wind forcing, eddy forcing, and topographic effects (Tansley and Marshall 2001, Gent *et al.* 2001), which makes them strongly dependent on wind forcing, with

a time scale possibly as short as 9 days (Clarke 1982). Yet we need OBCs to realistically simulate a basin like the South Atlantic. No simple alternative to this obstacle is available, as the problem is mathematically ill-posed (Bennett and Kloeden 1981). It is therefore important to keep in mind that a significant part of ocean sensitivity may be inhibited in regional models like this one.

North of $40°$S, permanent anticyclonic winds sustain the oceanic subtropical gyre along with downward Ekman pumping. On a seasonal mean time scale, the latter increases temperature at most by 0.2-$0.7°$C below the Ekman layer (5-th model level, yellow in Fig. 6b), but still by about 0.05-$0.1°$C at 400m depth, which remains significant as compared to our idealized observation error $0.02°$C at the same depth. On the other hand, subtropical regions are weakly influenced by OBCs, and thus the gyre barotropic flow becomes sensitive to wind forcing. On the seasonal mean time scale, the western boundary current's (WBC) transport is indeed changed by 7.5 Sv between $(+)$ and $(-)$ trajectories. Lastly, coastal upwelling occur along the Benguela and Brazil coasts.

The above discussion indicates that hydrological sensitivity to wind stress can be strong enough to be depicted by signals exceeding observational errors in our idealized context. There are thus good indications that our data might be appropriate to identify, at least partially, wind stress patterns by 4D-Var. The assimilation set-up is similar to the one for thermohaline flux experiments, with large constant background errors defined as four times the standard deviation of the true fluxes ($\sigma^b_{\boldsymbol{\tau}_x} = 4 \times 0.08 = 0.32$N.m^{-2}, $\sigma^b_{\boldsymbol{\tau}_y} = 4 \times 0.03 = 0.12$N.m^{-2}). Interestingly, we find that the seasonal mean wind stress is poorly retrieved by the assimilation system (Fig. 7a,b). The convergence was slow and required twice as many iterations as needed for estimating thermohaline fluxes to achieve an acceptable level of convergence. Most remarkably, the meridional stress $\boldsymbol{\tau}_y$ hardly deviates from its zero background value. The absence of a significant sensitivity of the mean hydrological fields with respect to meridional stress $\boldsymbol{\tau}_y$ alone (compared to observational error) might explain this failure. On the other hand, zonal wind stress $\boldsymbol{\tau}_x$ is unequally reconstructed over the basin. North of $45°$S, an excellent correlation of 0.96 is found with truth, thus demonstrating the ability of our system to extract Ekman pumping information from the data. This partial identifiability of the wind stress may be related to the Sverdrup equilibrium, which etablishes at mid latitudes a linear balance between the wind stress field and the meridional transport of water columns. The latter is indeed observed in our hydrographic data, via geostrophy. Consequently, the barotropic WBC is properly reconstructed. Furthermore, westward zonal wind stress patterns associated with upwellings in the Benguela and Brazil coastal regions have been correctly reconstructed as well (not shown). Reconstructed wind stress at latitudes higher than $66°$S also correlate well with truth (0.92), showing that the southern downwelling mechanism was properly captured by the system. By contrast, this correlation drops down to 0.53 within latitudes 40-$55°$S, because of erroneous estimated eastward wind stress. On the seasonal mean, the latter is incorrectly positioned as well as underestimated in strength and meridional extent.

From these results we conclude that the seasonal mean wind stress can not be fully identified by mean hydrological data, and that this problem is strongly ill-posed in our configuration. Recalling the sensitivity issue related to the OBC specification, one can argue that part of our conclusions are restricted to the scope of regional models like ours. This is not relevant to the $\boldsymbol{\tau}_y$ estimation problem however. In addition, it is likely that better background information might help to find the correct solution, which would be the case in realistic data assimilation experiments. However, it seems risky to

trust wind stress estimation by 4D-Var in our configuration, and this warning is largely corroborated by the results in the next section.

(*b*) *Simultaneous estimation of wind stress and thermohaline fluxes.*

By controlling all air-sea fluxes together, we can at best expect to reproduce the results from the separate identification experiments in the previous section. Joint estimation can thus *a priori* not give satisfactory results regarding wind stress forcing. The experiment (not shown) actually degrades the positive results acquired when only thermohaline fluxes were simultaneously identified, and none of the fields can be properly recovered. The large increase in the number of control parameters in the estimation problem thus leads to an ill-posed, physically underdetermined problem unless more appropriate information is given.

We have just shown that badly constrained degrees of freedom can prevent well constrained ones from being improved. We now illustrate how a perfectly known control variable, which is weakly constrained by the data, can be substantially degraded. In this experiment, wind stress along with heat fluxes $(Q, \boldsymbol{\tau}_x, \boldsymbol{\tau}_y)$ are estimated. Background winds stresses are chosen to be perfect, whereas heat fluxes are defined by austral autumn fields, introducing a seasonal shift in heat flux forcing with respect to the true fluxes which are defined by summer fields. In addition, the background error standard deviations are now smaller ($\sigma^b_Q = 80$W/m^2, $\sigma^b_{\boldsymbol{\tau}_x} = 0.08$N.m^{-2} and $\sigma^b_{\boldsymbol{\tau}_y} = 0.03$ =N.m^{-2}), which brings us closer to a realistic 4D-Var data assimilation experiment set-up. The estimated seasonal mean heat flux increment qualitatively agrees with truth (Fig. 8b), but is significantly underestimated by about 10 to 30W/m^2 (on zonal mean). At the same time, it is found that the wind stress is modified by a relative perturbation of 14% r.m.s., a noticeable degradation of the originally perfect field. The wind stress amplitude is reduced, and its maximum is shifted to the south (Fig. 8a). Thus, to warm up ocean surface temperatures, a reduction of northward Ekman heat advection takes place instead of enhanced positive heat flux into ocean. In other words, a heat flux estimation error is balanced by an unrealistic wind stress increment.

(*c*) *Discussion.*

In this section, we showed that coastal upwelling observations allow us to recover the generating wind stress. This could be partly expected since the associated hydrological perturbations are large, and since no other wind mechanisms are likely to generate them. An apparently stronger result is that the weak Ekman pumping signal observed in hydrology can also be converted into a zonal anticyclonic wind pattern. As in the thermohaline flux experiments, improved wind stresses should be obtained using a better background state and time-distributed data to introduce wind evolution information into the system. Howeverer, it is not obvious that our Ekman pumping result can apply to real data experiments. In the latter framework, observation (instrumental and representativeness) errors could make the upward pumping oceanic signal hardly discernable from the observations.

On the other hand, we demonstrated above the strong sensitivity of ocean surface currents to wind stress, which can be explained by analogy with the hydrology sensitivity to thermohaline fluxes. This suggests that surface current observations may therefore be more appropriate than hydrological data to identify wind stress forcing. Note that altimeter data would provide a constraint on the surface geostrophic currents. The latter is already implicitly used in hydrological data like ours, whereas wind induced Ekman

currents are ageostrophic. Hence altimeter derived surface current data are probably not appropriate to the wind stress inverse estimation problem.

We recommend therefore to take extra care when controlling wind stress forcing, unless available data have explicitly been shown appropriate for this task. Note however that improving the wind stress is probably not as crucial to ocean modelling as improving the thermohaline fluxes, since satellite scatterometers provide wind fields of relatively high quality while heat and freshwater fluxes are either calculated by help of bulk formulae with large uncertainties or taken from atmospheric models where they are generally known to be poorly reliable.

5. SUMMARY AND CONCLUDING REMARKS

(*a*) *Summary*

In this paper, we have investigated a method for estimating air-sea fluxes from ocean data, which does not require the use of bulk formulae and can take observation and background errors into account. More precisely, we have been concerned with the identifiability of climatological forcing fluxes using seasonal hydrological data, in an idealized framework where data are perfect with respect to the ocean model and where all estimated fields have a known true value. The estimation procedure relied on a 4D-Var algorithm, which makes use of the adjoint of a primitive equation ocean model to minimize a cost function measuring the distance between observational and model information. Monthly mean forcings were taken as control variables, and the ability of the assimilation system to retrieve them at different time scales (seasonal, monthly) by use of our data was discussed. A stringent framework was chosen, where no useful *a priori* information about fluxes was assumed available. At the same time, data were perfect with respect to the model dynamics, and no simulated observational noise was added to them. Other model parameters, such as initial conditions and open boundary forcings, were also assumed perfectly known.

The ocean sensitivity of the model equivalent to the observations with respect to the surface fluxes was first explored. The stronger this sensitivity, the better the identifiability of the fluxes from the data. It was found that the seasonal mean heat and freshwater fluxes could be identifiable by such data, regardless of whether they were estimated separately or jointly. The associated intraseasonal variability was partially recovered. This was particularly surprising since the data were seasonally averaged, and was attributed to the dynamical evolution constraints enforced by the OGCM within the cost function. Data with higher temporal sampling would be necessary to improve the intraseasonal retrieval. These results demonstrate nonetheless that it would be meaningful to control the thermohaline fluxes when moving to real data experiments.

By contrast, the wind stress was poorly estimated from hydrographic data. Seasonal mean zonal stress could be properly recovered in the subtropical gyre and in coastal upwelling areas, whereas the westerly winds were erroneously reconstructed. Furthermore, meridional stress could not be recovered, even partially. It was suggested that the failure to estimate westerly winds might be an artifact of the open boundary specification, which artificially removes any barotropic sensitivity to wind forcing in the ACC area. This points out that regional models, though necessary for many applications, may give rise to a number of critical issues that we must be aware of. In addition, it was suggested that upper ocean current observations might be more appropriate to wind stress estimation than hydrological data.

Whenever wind stress was estimated, the assimilation system was unable to recover the true solution, and convergence was difficult to achieve. A perfectly known background wind stress field was even shown to be significantly degraded in order to balance a heat flux estimation error. This showed that in our setting, the inverse wind stress estimation problem is physically ill-posed, even though by introducing a background term it always possesses a mathematical answer. In other words, different forcing fields can drive the ocean model close to the observations (in the sense of Eq. 5), because of the nullspace of the linearized operator **G** which inhibits identifiability. Not enough information is given to the system to allow it to distinguish between possible solutions, and further examination of optimal cost values (not shown) reveals that a minimal norm solution can be picked out, as enforced by the background term.

(*b*) *Concluding remarks*

Some of our conclusions related to OBCs suggest that it would be worth estimating open boundary parameters. Optimizing hydrological fields along open boundaries can indeed prove beneficial in real data experiments if the prescribed fields are not fully compatible with interior observations (Deltel 2002). In our configuration, improved fields of this kind only have a local impact restricted to the neighboorhood of OBCs, since the advective scale due to ACC over one season does not exceed a few hundred kilometers. On the other hand, one may be tempted to also optimize prescribed barotropic fields, like the ACC transport. Such corrections can again improve consistency with interior data, and would impact the whole basin. However, the results of Zhang and Marotzke (1999) and Ferron and Marotzke (2001) suggest, in a similar framework, that hydrographic data badly constrain boundary velocities. Moreover, estimating these fields can not be helpful in the wind stress identification process, unless they become prognostic variables instead of being introduced as forcings.

On the other hand, when estimated in this study, all background forcing errors were assumed to be mutually uncorrelated, which is a crude approximation to reality. Actual correlations result from a complex balance, and are difficult to specify. The ocean was also considered to be purely forced by the atmosphere, so that no coupling processes between the two fluids were involved. Relaxing these assumptions was beyond the scope of this paper.

Another limitation of this study is that we have been investigating only the austral summer season, restricted to the South Atlantic basin. Therefore, our findings cannot probably be extended to strong winter cooling events with associated oceanic convection, or to very different dynamical regimes like those in the equatorial area, which both deserve specific investigation.

An important issue raised by simultaneous estimation of initial conditions and forcings is that the number of control parameters would be significantly increased. One can wonder whether the assimilation system could then discriminate, within the data, relevant contributions to both substantially different control sets. Our results demonstrate that the system might erroneously attribute, for example, the Ekman pumping signal to an initial condition misspecification instead of wind stress error, because of relative sensitivity reasons. Note that a long enough assimilation window could help separate out these contributions, since only the initial ocean trajectory is probably most sensitive to initial conditions whereas forcings control the model trajectory at later times (Bonekamp *et al.* 2001). However, in their 1D twin data 4D-Var experiments, Zhu *et al.* (2002) successfully estimate initial conditions along with heat flux (over 7 days), which provides an indication that this procedure might work in a more general OGCM context, at least whenever oceanic advection remains weak.

To conclude, we recall that our OGCM was applied as a strong constraint, and that neither observational noise nor representativeness error were added to the data. A weakness when extrapolating our estimation approach to real data experiments is that the model strong constraint hypothesis would be violated. In addition, the observation error covariance matrix **R** would need to be revisited. Observational errors would be significantly larger, and the complicated error correlation structures introduced by objective mapping to construct a climatological hydrographic database could need to be accounted for, to avoid overweighting individual observations (Daley 1991). A weak constraint approach would make it possible to explicitly take model error into account within the variational framework (Bennett and Thorburn 1992, Courtier 1997, Bennett *et al.* 1998, Bennett *et al.* 2000). However this would largely increase the underdeterminacy of the problem, which is obviously not affordable with a dataset like ours, and may also be impractical with currently available oceanic observations.

6. FIGURES

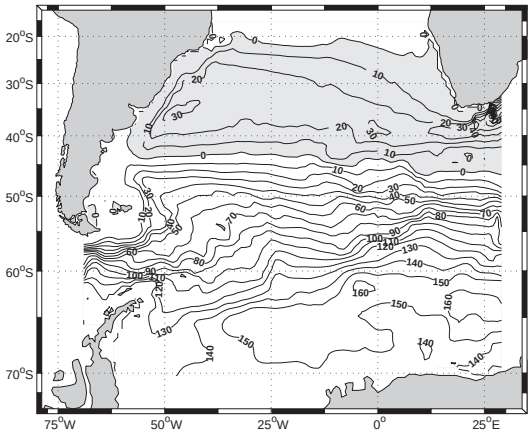

Figure 1. Mean stream function of the spin-up simulation (Unit: Sverdrup, contouring interval: 10 Sv)

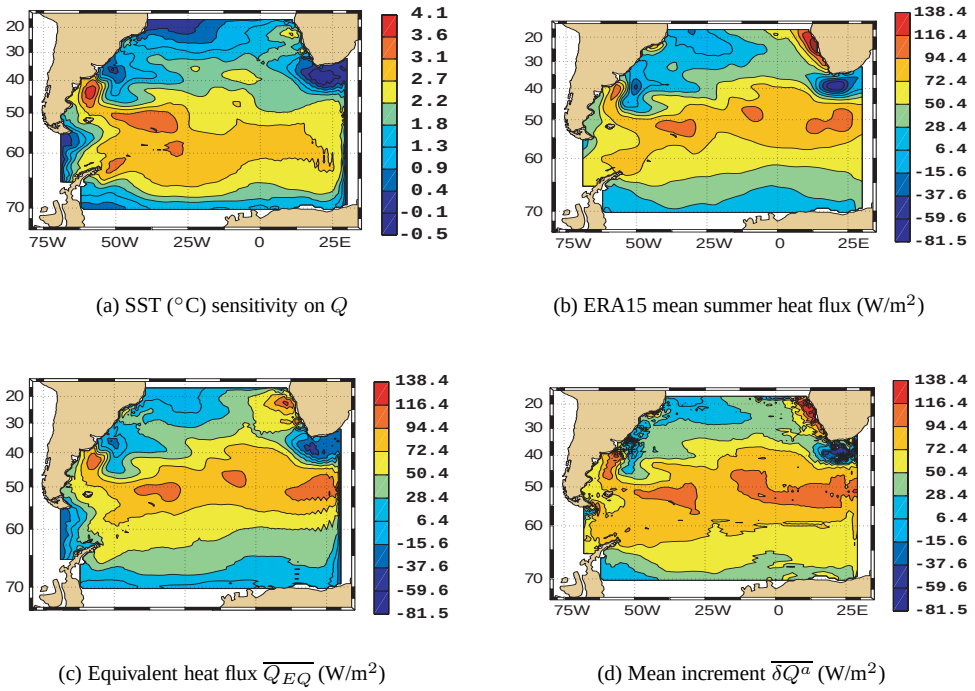

(a) SST (°C) sensitivity on Q

(b) ERA15 mean summer heat flux (W/m^2)

(c) Equivalent heat flux $\overline{Q_{EQ}}$ (W/m^2)

(d) Mean increment $\overline{\delta Q^a}$ (W/m^2)

Figure 2. The surface mean SST impact (a) (denoted by $\overline{\theta^+} - \overline{\theta^-}$ in the text) of the ERA15 heat flux forcing (b). The mean heat flux inverse estimation by (c) thermal content and (d) 4D-Var methods.

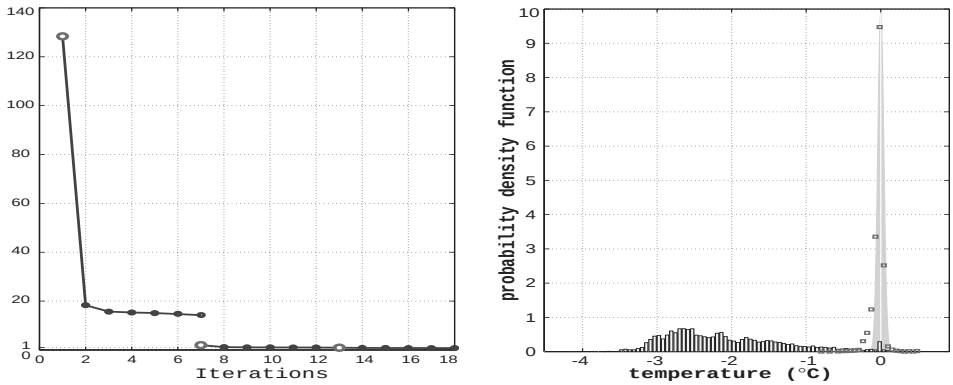

(a) Cost function

(b) Surface temperature residuals distribution

Figure 3. Convergence and residuals: The cost function (a) is scaled by $2/p$ to have the unity mathematical expectation. Large circles indicate outer loops. The surface temperature residuals are illustrated in (b). The squares show the distribution of residuals after assimilation, whereas the histogram depicts the background departures and the light grey Gaussian shape shows the observation error probability density function.

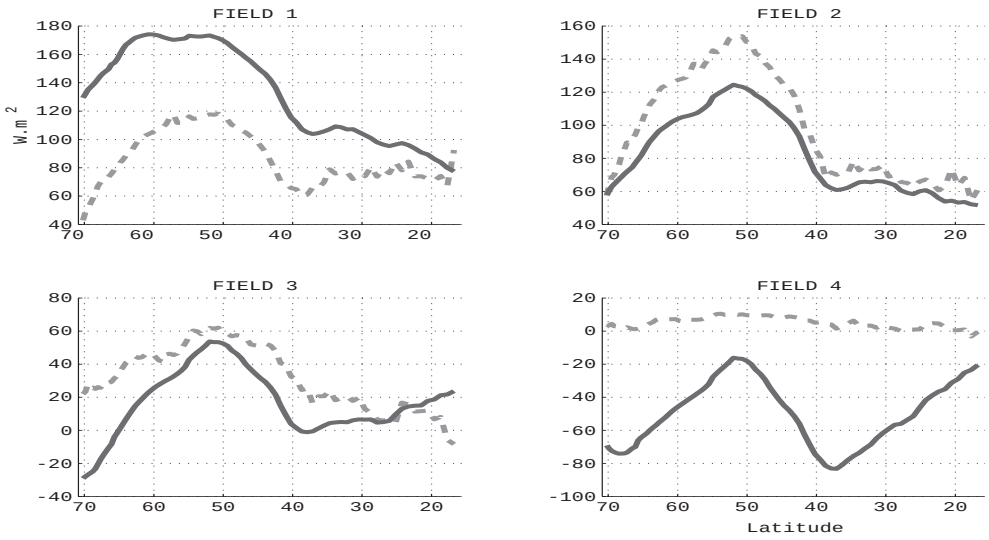

Figure 4. The intraseasonal history of δQ^a (zonal means) as reconstructed by 4D-Var. Solid lines show the true heat flux; dashed lines show the estimated heat flux. The background state δQ^b is zero.

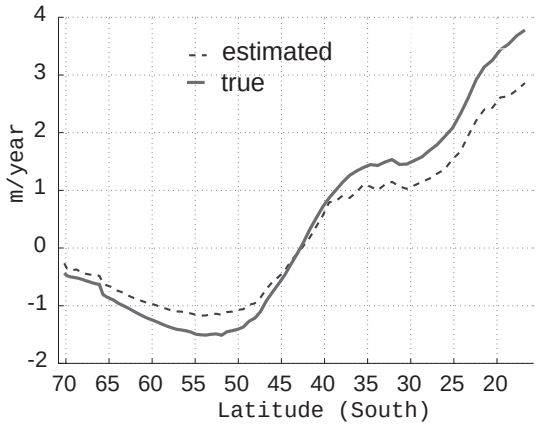

Figure 5. Seasonal freshwater flux $E - P$ (zonal mean): the dashed line shows the 4D-Var estimation; the solid line illustrates the true field. The background state $(E - P)^b$ is zero.

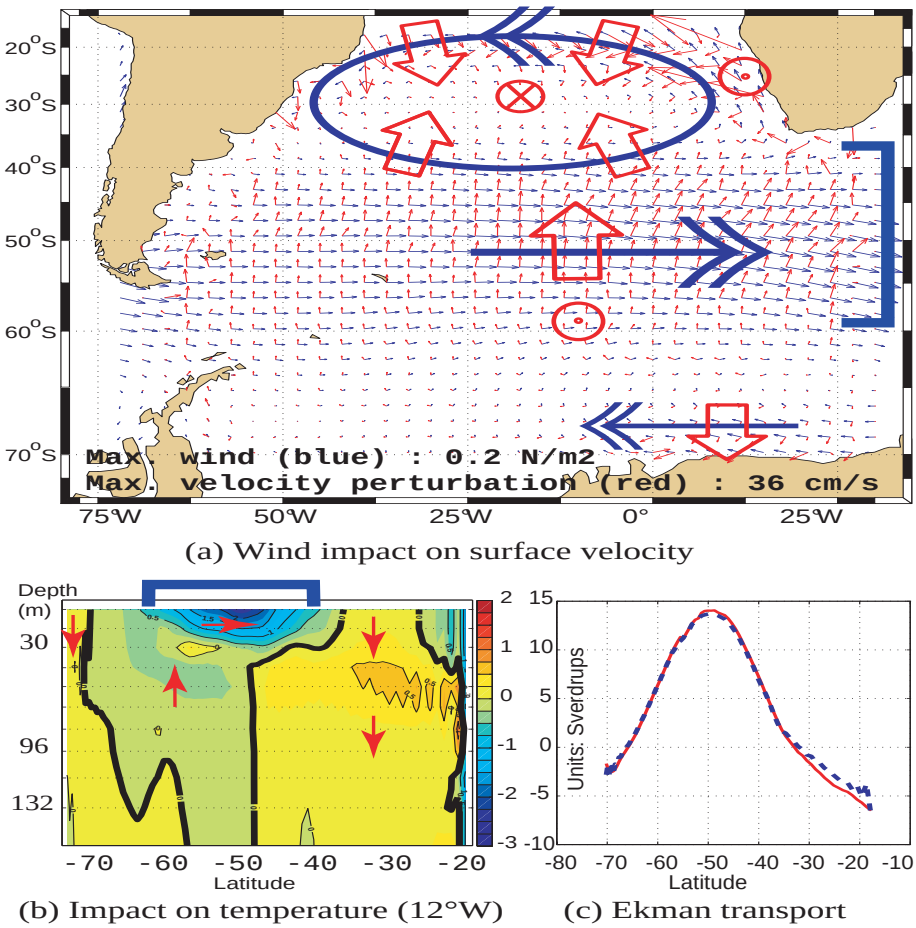

Figure 6. Sensitivity to wind stress forcing. In (a), the mean wind stress field (blue) is represented along with its impact on surface currents (red) integrated over the Ekman layer depth (3 model levels). Cross section of temperature (°C) along 12°W is shown in (b). The wind stress impact on the Ekman layer meridional transport is shown in (c) (dashed line), along with the corresponding theoretical Ekman tranport (solid line).

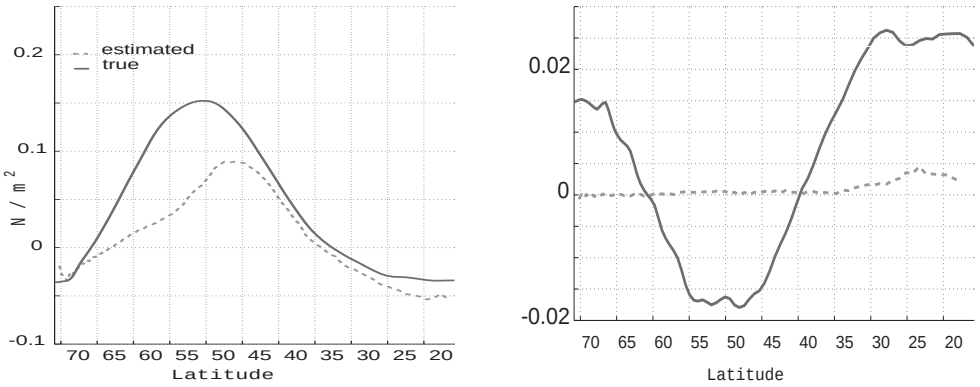

(a) Zonal mean of $\boldsymbol{\tau}_x$

(b) Zonal mean of $\boldsymbol{\tau}_y$

Figure 7. Identifiability of wind stress. The seasonal mean zonal and meridional stresses are illustrated in (a) and (b) (zonal means). The true wind stress (solid line) can be compared to the wind stress reconstructed by 4D-Var after 36 iterations (dashed line). The background state $\boldsymbol{\tau}^b$ is zero.

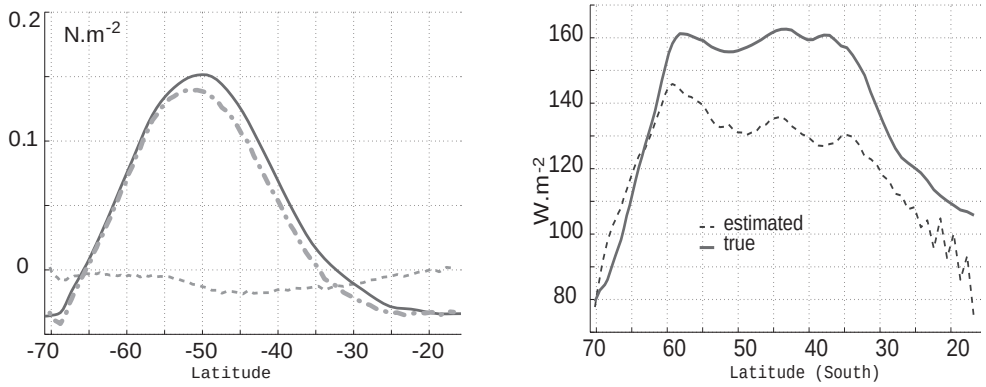

(a) Zonal mean of $\boldsymbol{\tau}_x$

(b) Zonal mean of Q

Figure 8. Heat flux identifiability when the wind stress is also estimated (initially perfect, but free to adjust). The background heat flux is no longer zero, but defined by autumn fields. Zonal wind stress is represented in (a): true field (solid); 4D-Var estimated optimal stress (dash-dotted line); and the corresponding assimilation increment. True and 4D-Var estimated heat fluxes are represented in (b).

REFERENCES

Barnier, B., Marchesiello, P., De Miranda, A. P., Coulibaly, M. and Molines, J. M. 1998 A "sigma" coordinate primitive equation model for studying the circulation in the south Atlantic. Part I : Model configuration with error estimates, *Deep Sea Res.*, **45,** 543–572

Bennett, A. and Thorburn, M. 1992 The generalized inverse of a nonlinear quasigeostrophic ocean circulation model, *J. Phys. Oceanogr.*, **22,** 213–230

Bennett, A., Chua, B., Harrison, D. and McPhaden, M. 1998 Generalized inversion of tropical atmosphere-ocean data and a coupled model of the tropical pacific, *J. Climate*, **11,** 1768–1792

Bennett, A., Chua, B., Harrison, D. and McPhaden, M. 2000 Generalized inversion of tropical atmosphere-ocean data and a coupled model of the tropical pacific. Part II: The 1995-96 la nina and 1997-98 El Nino, *J. Climate*, **13,** 2770–2785

Bennett, A. F. and Kloeden, P. E. 1981 The ill-posedness of open ocean models, *J. Phys. Oceanogr.* **11,** 1027–1029

Blanke, B. and Delecluse, P. 1993 Variability of the tropical Atlantic ocean simulated by a general circulation model with two different mixed layer physics, *Q. J. R. Meteorol. Soc.*, **23,** 1363–1388

Bonekamp, H., van Oldenborgh, G. J. and Burgers, G. 2001 Variational assimilation of tropical ocean-atmosphere and expandable bathythermograph data in the Hamburg ocean primitive equation ocean general model, adjusting surface fluxes in the tropical ocean, *J. Geophys. Res.*, **106,** 16693–16709

Bryson, A. and Ho, Y. 1975 Applied Optimal Control, *New York: Hemisphere*

Chavent, G. 1979 Identification of distributed parameter systems : about the least squares methods, its implementation and identifiability, *Proc. 5th Symp. in Identifiability and System Parameter Estimation, Darmstadt, Pergamon Press, Oxford*, 85–87

Clarke, A. 1982 The dynamics of large-scale, wind-driven variations in the Antarctic circumpolar current, *J. Phys. Oceanogr.*, **12,** 1092–1105

CLIPPER Scientific Team 2001 Modélisation à haute résolution de la circulation dans l'océan Atlantique forcée et couplée océan-atmosphère, *Rapport Scientifique et Technique, N° Clipper-R1-2001, LEGI/LPO/LODYC/LEGOS*

Courtier, P. 1997 Dual formulation of four-dimensional variational assimilation, *Q. J. R. Meteorol. Soc.*, **123,** 2449–2461

Courtier, P, Thépaut, J.-N. and Hollingsworth, A. 1994 A strategy for operational implementation of 4d-var, using an incremental approach, *Q. J. R. Meteorol. Soc.*, **120,** 1367–1387

Daley, R. 1991 Atmospheric Data Analysis, *Cambridge Atmospheric and Space Science Series*, Cambridge University Press, Cambridge, UK, 457 pp.

Deltel, C. 2002 'Estimation de la circulation dans l'océan Atlantique sud par assimilation variationnelle de données in situ. Impact du contrôle optimal des forçages et de l'hydrologie aux frontières ouvertes', *PhD thesis, Univ. de Bretagne Occidentale*, 185 pp.

Ferron, B. and Marotzke, J. 2001 Impact of 4d-variational assimilation of WOCE hydrography on the meridional circulation of the Indian ocean, *Deep Sea Res. II*, **50 (12/13),** 2005–2021

Font, J., Kerr, Y. and Berger, M. 2000 Measuring ocean salinity from space : the European Space Agency's SMOS mission, *Backscatter*, **11,** 17–19

Garnier, E., Barnier, B, Siefridt, L. and Béranger, K. 2000 Investigating the 15 years air-sea flux climatology from the ECMWF re-analysis project as a surface boundary condition for ocean models, *Int. J. Climatology*, **20,** 1653–1673

Gaspar, P., André, J.-C. and Lefevre, J. 1990 The determination of latent and sensible heat fluxes at the ocean-atmosphere interface viewed as an inverse problem, *J. Geophys. Res.*, **95,** 16169–16178

Gent, P. R., Large, W. G. and Bryan, F. O. 2001 What sets the mean transport through Drake passage?, *J. Geophys. Res.*, **106,** 2693–2712

Gibson, J. K., Kallberg, P., Uppala, S., Noumura, A, Hernandez, A. and Serrano, E 1997 ERA description, *ECMWF Re-Analysis Project Report Series, ECMWF, Reading, UK*, 77pp.

Goodson, R. E. and Polis, M. P.	1979	Parameter identification in distributed systems: a synthesizing overview in identification of parameters in distributed systems, *Symposium of Annual Aut. Control. Am. Soc. Mech. Eng., New York*, 1–31
Ide, K., Courtier, P., Ghil, M. and Lorenc, A.	1997	Unified notation for data assimilation: operational, sequential and variational, *J. of Meteorol. Soc. of Japan*, **75,** 181–189
Kitamura, S. and Nakarigi, S.	1977	Identifiability of spatially-varying and constant parameters in distributed systems of parabolic type, *SIAM J. Control. Optim.*, 785–802
Lorenc, A.	1986	Analysis methods for numerical weather prediction, *Q. J. R. Meteorol. Soc.*, **112,** 1177–1194
Madec, G., Delecluse, P., Imbard, M. and Lévy, C.	1998	OPA 8.1 ocean general circulation model reference manual, *Note N° 11 du Pôle de Modélisation de l'IPSL*,
Navon, I. M.	1997	Practical and theoretical aspects of adjoint parameter estimation and identifiability in meteorology and oceanography, *Dyn. Atmos. Oceans*, **27,** 55–79
Reynaud, T., LeGrand, P., Mercier, H., and Barnier, B.	1998	A new analysis of hydrographic data in the Atlantic and its application to an inverse modelling study, *International WOCE Newsletter*, **32,** 29–31
Roquet, H., Planton, S. and Gaspar, P.	1993	Determination of ocean surface heat fluxes by a variational method, *J. Geophys. Res.*, **98,** 10211–10221
Stammer, D., Wunsch, C., Giering, R., Eckert, C., Heimbach, P., Marotzke, J., Adcroft, A., Hill, C. and Marshall, J.	2002	Global ocean circulation during 1992-1997, estimated from ocean observations and a general circulation model, *J. Geophys. Res.*, **107,** C9 3118, doi:10.1029/2001JC000888
Talagrand, O.	1998	A posteriori evaluation and verification of analysis and assimilation algorithms, *ECMWF Workshop on diagnosis of data assimilation systems*, 17–28
Tansley, C. E. and Marshall, D. P.	2001	On the dynamics of wind-driven circumpolar currents, *J. Phys. Oceanogr.*, **31,** 3258–3273
Tichonov, A. N.	1963	Regularization of ill posed problems, *Dokd. Akad. Nauk., USSR 153*, 49–52
Treguier, A.-M., Barnier, B., de Miranda, A., Molines, J.-M., Grima, N., Imbard, M., Madec, G., Messager, C. and Michel, S.	2001	An eddy permitting model of the Atlantic circulation: Evaluating open boundary conditions, *J. Geophys. Res.*, **106,** 22115–22129
Weaver, A. T. and Courtier, P.	2001	Correlation modelling on the sphere using a generalized diffusion equation, *Q. J. R. Meteorol. Soc.*, **127,** 1815–1846
Weaver, A. T., Vialard, J. and Anderson, D. L. T.	2003	Three- and four-dimensional variational assimilation with a general circulation model of the tropical pacific ocean. Part I: Formulation, internal diagnostics, and consistency checks, *Mon. Weather Rev.*, **131,** 1360–1378
Yuan, D. and Hsueh, Y.	1998	Inverse determination of surface heat flux over the Yellow sea in winter of 1986 from sea surface temperature data, *J. Phys. Oceanogr.*, **28,** 984–990
Yuan, D. and Rienecker, M	2003	Inverse estimation of sea surface heat flux over the equatorial Pacific ocean: seasonal cycle, *J. Geophys. Res.*, **108,** C8 3247, doi:10.1029/2002JC001367
Zhang, K. and Marotzke, J.	1999	The importance of open-boundary estimation for an Indian ocean gcm-data synthesis, *J. Mar. Res.*, **57,** 305–334
Zhu, J., Kamachi, M. and Wang, D.	2002	Estimation of air-sea flux from ocean measurements : an ill-posed problem, *J. Geophys. Res.*, **107,** C10 3159, doi:10.1029/2001JC000995